Patterning of Nanoporous Anodic Aluminum Oxide Arrays by Using Sol−Gel Processing, Photolithography, and Plasma Etching

Dmitri A. Brevnov,[†] Marcos Barela,[†] Menake E. Piyasena,[‡] Gabriel P. López,[†,‡] and Plamen B. Atanassov*[,†]

Department of Chemical and Nuclear Engineering and Department of Chemistry, Center for Micro-Engineered Materials, The University of New Mexico, Albuquerque, New Mexico 87131

Received June 30, 2003. Revised Manuscript Received December 9, 2003

Patterned anodic aluminum oxide (AAO) arrays were fabricated by using sol−gel processing, photolithography, plasma etching, and two-step anodization. The fabrication process included the following general steps. First, a layer of aluminum was evaporated onto silicon wafers. Second, a silica layer was deposited by spin-coating a sol. Next, a patterned layer of a photoresist was deposited by standard photolithographic procedures. Subsequently, the pattern of photoresist was transferred to the underlying layer of silica by fluorocarbon plasma etching. Finally, AAO arrays were formed by the two-step anodization of exposed aluminum (e.g., not covered by silica). Deposition and etching of the silica layer were monitored by spectroscopic ellipsometry. Electrical measurements were performed to investigate the ability of the silica layer to act as a barrier that prevents anodization of aluminum. The structure of patterned AAO arrays was studied by scanning electron microscopy. A clear boundary was observed between two regions. The first region, nanoporous AAO, had pores arranged in an approximately hexagonal order, whereas the second region, aluminum covered with silica, contained no pores. The patterned AAO arrays have two key advantages over other AAO arrays. These arrays exhibit enhanced mechanical strength and possess electrical conductivity, due to the incorporation of regions of aluminum. In addition, the reported fabrication method allows formation of the nanoporous alumina patterns on the microscopic length scale. All the fabrication steps can be integrated into a suitable fabrication line, because they are carried out using standard microfabrication tools. These properties and advantages will facilitate the incorporation of patterned AAO arrays into micro- and nanodevices.

Introduction

Anodic aluminum oxide (AAO) membranes in the form of self-ordered nanoporous arrays are attractive for many technical applications in the rapidly growing nanotechnology field.[1−4] AAO membranes have been shown to serve as templates for fabrication of diverse nanostructures and membranes from other materials (e.g., polymers and metals).[1,2] Modification of the AAO membrane pores with metals or semiconductor materials will be useful for the fabrication of novel materials and devices with new properties and functions. This modification can be accomplished by a number of methods, including electro[5−7] and electroless[8] deposition, chemical vapor deposition,[9] sol−gel deposition,[10] and others. In addition, AAO membranes can be fabricated with a very high aspect ratio of pores. All of these properties make these nanoporous arrays very promising for application in design of new nanotechnology products, such as sensing devices, adsorbers, preconcentrators, gas and liquid transport fields, or membranes in microreactors or micropower sources.

The method to fabricate the nanoporous AAO arrays is straightforward, and the structure of aluminum/alumina/electrolyte interface during porous-type anodization in acidic electrolytes is well established.[11] This interface consists of three distinct layers: aluminum metal, a thin barrier oxide layer, and a relatively thick porous oxide layer. The electrochemical reaction (oxidation of aluminum to produce Al_2O_3), takes place at the aluminum metal/barrier oxide layer interface. The

* To whom correspondence should be addressed. E-mail: plamen@unm.edu.
[†] Department of Chemical and Nuclear Engineering.
[‡] Department of Chemistry.

(1) Martin, C. R. *Chem. Mater.* **1996**, *8*, 1739.
(2) Hoyer, P.; Nishio, K.; Masuda, H. *Thin Solid Films* **1996**, *286*, 88.
(3) Schmid, G. *J. Mater. Chem.* **2002**, *12*, 1231.
(4) Li, F.; Zhang, L.; Metzger, R. M. *Chem. Mater.* **1998**, *10*, 2470.
(5) Muller, F.; Muller, A.-D.; Kroll, M. Schmid, G. *Appl. Surf. Sci.* **2001**, *171*, 125.
(6) Chu, S.-Z.; Wada, K.; Inoue, S.; Todoroki, S.-i.; Takahashi, Y. K.; Hono, K. *Chem. Mater.* **2002**, *14*, 4595.
(7) Martin, B. R.; Dermody, D. J.; Reiss, B. D.; Fang, M.; Luon, A.; Natan, M. J.; Mallouk, T. E. *Adv. Mater.* **1999**, *11*, 1021.
(8) Menon, V. P.; Martin, C. R. *Anal. Chem.* **1995**, *6*, 7, 1920.
(9) Shelimov, K. B.; Davydov, D. N.; Moskovits, M. *Appl. Phys. Lett.* **2000**, *77*, 1722.
(10) Chu, S.-Z.; Wada, K.; Inoue, S.; Todoroki, S.-i. *Chem. Mater.* **2002**, *14*, 266.
(11) Despic, A.; Parkhutik, V. In *Modern Aspects of Electrochemistry*; Bokris, J. O'M., White, R. E., Conway, B. E., Eds.; Plenum Press: New York, 1989; No. 23, pp 401−493.

10.1021/cm034553v CCC: $27.50
Published on Web 01/28/2004

thickness of the barrier oxide layer depends linearly upon the anodization voltage. During anodization at a constant voltage, the thickness of the barrier oxide layer remains constant, because the rate of alumina dissolution on the electrolyte side is equal to the rate of alumina production on the metal side. The structure of the aluminum/alumina/electrolyte interface can be nondestructively investigated by electrochemical impedance spectroscopy (EIS) and spectroscopic ellipsometry (SE).[12] Whereas EIS is sensitive to only the dielectric properties of the barrier oxide layer, SE provides information about both the porous and barrier oxide layers.[12,13]

AAO arrays can be fabricated either on solid supports such as silicon wafers with aluminum films[13,14] or from bulk aluminum sheets (foil).[1,4] Free-standing AAO membranes are usually obtained when the underlying aluminum support is removed. Despite many attractive features, free-standing AAO membranes have drawbacks that currently limit their facile integration into micro- and nanodevices. These drawbacks include a lack of electrical conductivity and low mechanical strength. The electrical conductivity is necessary, for example, for the design of preconcentrators. The fragility of AAO membranes is a severe shortcoming for the fabrication of AAO MEMS. To provide electrical conductivity and improve mechanical strength, we have fabricated AAO arrays composed of separate regions of nanoporous aluminum oxide and aluminum.[15] In this case, the aluminum features reinforce the fragile alumina layer while also providing electrical contact with the underlying aluminum substrate.

In this report, we show the application of sol−gel processing, photolithography, plasma etching, and a two-step anodization procedure[16] to fabricate the patterned AAO arrays. Silica films have been conveniently and reproducibly deposited on flat surfaces using the sol−gel process.[17,18] Photolithography and plasma etching are frequently used to transfer patterns from a layer of photoresist to an underlying layer. The two-step anodization procedure has been previously demonstrated to result in ordered nanoporous anodic aluminum oxide arrays.[16] Thus, the approach, which is reported here and employed for patterning of AAO arrays, combines advantages and practical utilities of well-established methods and protocols of sol−gel chemistry, photolithography, plasma etching, and anodization of aluminum in acidic electrolytes.

For successful implementation of this approach, it is critical that the patterned silica layer blocks the formation of pores in the underlying layer of aluminum. To address this issue, we employ spectroscopic ellipsometry (SE) to measure the thickness of silica layers after deposition and thermal annealing, and during plasma etching. In addition, electrochemical measurements are carried out in order to determine whether the deposited silica layer can act as an effective dielectric barrier under severe oxidative conditions in the electrochemical cell. A combination of these measurements allows us to conclude whether the silica layer prevents the formation of pores during anodization of aluminum.

Experimental Section

All chemicals, unless specified otherwise, were obtained from Aldrich Chemical Co. (St. Louis, MO) and were used without further purification. Silicon wafers with a 300-nm layer of evaporated aluminum were obtained from Micromachines Inc. (Monrovia, CA). The wafers were diamond-scribed into 2-cm-wide squares and used for further processing. A silica layer was deposited on the evaporated aluminum film by a sol−gel protocol. The procedure to prepare the sol solution that results in the silica films with minimal porosity is adopted with modification from elsewhere.[17] A stock solution was typically prepared by refluxing a mixture of tetraethyl orthosilicate (TEOS), ethanol, deionized water, and dilute HCl (mole fractions 1:3.8:1:0.0005) at 60 °C for 90 min.[19] To prepare a sol, the stock solution was diluted with ethanol, 0.07 M HCl, and deionized water in the ratio 1:2:0.1:0.1. An aliquot fraction of 100 μL of the prepared sol was deposited onto slides with a surface area of approximately 4 cm^2 by spin coating at 800 rpm for 40 s. Thermal annealing was performed overnight (for approximately 10−12 h) at 250 °C in an air atmosphere. The thickness of the resulting silica layer was measured by SE immediately after spin coating and after thermal annealing. Single angle (70.0°) SE experiments and data analysis were performed with a M-44 ellipsometer (J. A. Woollam Co., Inc.) and WVASE32 software. Forty-four pairs of ψ and Δ were collected over a wavelength range from 418 to 753 nm.

Standard photolithographic procedures (e.g. spin coating, soft bake, exposure, postexposure bake, and development) were employed to create patterns on the surface of silica-coated slides. A 10-μm layer of the epoxy-based negative photoresist SU-8 25 (Microchem Corp., Newton, MA)[20] was deposited onto slides by spin coating initially at 500 rpm for 10 s and then at 3000 rpm for 40 s. Next, the slides were baked at 75 °C for 10 min and left in the dark for a further 30 min at room temperature. The photomask, a high-resolution transparency (3300 dpi), had a pattern of two perpendicular lines 0.25 mm wide. The design on the photomask was contact-printed onto the photoresist-coated slide by exposure to UV radiation at 365 nm for 10 min followed by another 20 min in the dark. The slides were then baked at 75 °C for 10 min and left in the dark for another 20 min at room temperature. Finally, the unexposed (not cross-linked) photoresist was removed by developing the slides in SU-8 developer (Microchem. Corp., Newton, MA).

The pattern of photoresist was transferred to the underlying layer of silica by plasma etching. The inductively coupled plasma reactor used to pattern the silica layer was a modified Gaseous Electronics Conference Reference Cell described in detail elsewhere.[21] Briefly, the reactor was a stainless steel vacuum processing chamber with a base pressure of 10^{-5} Torr. The inductively coupled source, a five-turn planar coil located on the top of the chamber, was powered by a 0−1000 W ENI radio frequency power supply at 13.56 MHz. Coupling was achieved through a quartz dielectric window. The sample was placed 6 cm below the dielectric window on an electrode powered by a ENI 0−500 W radio frequency power supply. The pattern transfer was performed in a CF_4 plasma maintained at 20 mTorr total pressure, 575 W source power, and

(12) De Laet, J.; Terryn, H.; Vereecken, J. *Electrochim. Acta* **1996**, *41*, 1155.
(13) Brevnov, D. A.; Rama Rao, G. V.; López, G. P.; Atanassov, P. B. *Electrochem. Acta*, submitted for publication.
(14) Crouse, D.; Lo, Y.-H.; Miller, E.; Crouse, M. *Appl. Phys. Lett.* **2000**, *76*, 49.
(15) Yan, J.; Rama Rao, G. V.; Barela, M.; Brevnov, D. A.; Jiang, Y.; Xu, H.; López, G. P.; Atanassov, P. B. *Adv. Mater.* **2003**, *15*, 2015.
(16) Masuda, H.; Satoh, M. *Jpn. J. Appl. Phys.* **1996**, *35*, L126.
(17) Brinker, C J.; Scherer, G. W. *Sol−gel Science: The Physics and Chemistry of Sol−gel processing*; Academic Press: New York, 1990.
(18) Hench, L.; West, J. K. *Chem. Rev.* **1990**, *90*, 32.
(19) Rama Rao, G. V.; López, G. P.; Bravo, J.; Pham, H.; Datye, A. K.; Xu, H.; Ward, T. L. *Adv. Mater.* **2002**, *14*, 1301.
(20) MicroChem Corp.; www.microchem.com.
(21) Miller, P. A.; Hebner, G. A.; Greenberg, K. E.; Pochan, P. D.; Aragon, B. P. *J. Res. Natl. Inst. Stand. Technol.* **1995**, *100*, 427.

100 W bias power. The rate at which the exposed silica layer was removed was determined by SE measurements.

Before anodization, slides were treated with a 0.5 M solution of NaOH for 30 s to remove any residual silica in unexposed areas and then thoroughly washed with deionized water. These operations were repeated twice. Anodization of aluminum films with the patterned layers of the photoresist and silica was carried out in a 3 wt % solution of oxalic acid by using an in-house designed two-electrode cell thermostated at 0−1 °C.[13] The cell allowed exposure of a flat electrode with a geometric surface area of 1.4 cm^2 as defined by a rubber O-ring sealing. The electrical contact was made to the aluminum layer. A high-surface-area platinum mesh served as a counter electrode. To dissipate the heat generated during anodization, the electrolyte solution was constantly stirred during anodization by bubbling of a gas (nitrogen) through the cell. A computer-controlled Hewlett-Packard 4140B pA meter/DC voltage source was used to apply a ramp of 1.0 V/s for 30 s (in order to avoid a current overload) and then a DC voltage of 30 V for anodization. A two-step procedure was applied to grow ordered porous alumina films.[16] The first anodization was performed for 5 min. Etching of alumina was then performed in a mixture of 0.4 M phosphoric and 0.3 M chromic acids. During etching, the electrochemical cell was disconnected from electronic instrumentation and placed in a 70 °C oven for 25 min. The mixed acid temperature measured after the cell was removed from the oven was approximately 45 °C. An etching time of 25 min was considered to be sufficient to dissolve both porous and barrier alumina layers formed during the first anodization step.[12] The second anodization was performed under the same conditions as the first one, but lasted typically 10−15 min. At this time almost all of the exposed (not covered with silica) aluminum was converted into oxide film. The thin layer of aluminum is believed to be necessary for adhesion of nanoporous alumina to the silicon wafers.[22] Upon completion of the second anodization, the vertical structure in the areas not covered with silica consisted of three layers on the silicon substrate: porous aluminum oxide, barrier aluminum oxide, and aluminum, while the areas covered with silica remained pure aluminum. The surface morphology of patterned, anodic aluminum oxide slides was evaluated by a Hitachi (S-800) scanning electron microscope (SEM).

Results and Discussion

Figure 1 shows a block diagram of the overall process employed to fabricate patterned AAO membranes. The diagram includes the following steps: (1) a layer of aluminum is thermally evaporated on a silicon wafer; (2) a silica layer is deposited by spin coating a sol and thermal annealing at 250 °C; (3−5), standard photolithographic procedures (e.g., spin coating, soft bake, exposure, postexposure bake, and development) are employed to create the patterned layer of a photoresist; (6) the pattern of photoresist is transferred to the underlying layer of silica by fluorocarbon plasma etching of silica in the region with no photoresist; and (7) the two-step anodization procedure is applied to anodize aluminum in those areas that are not covered by the patterned layer of silica.

Figure 2 shows an ellipsometric spectrum (ψ and Δ) acquired after spin coating of a silica film on a piece of wafer before thermal annealing. The interference oscillations in ψ and Δ indicate the formation of a transparent silica film on the top of the aluminum. To reliably interpret the acquired ellipsometric measurements,

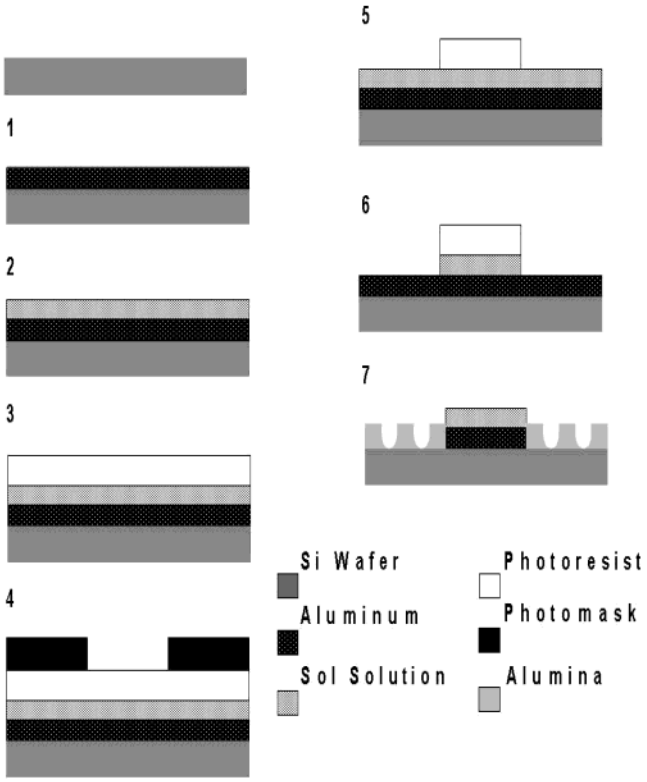

Figure 1. Schematic representation of the overall process employed to fabricate the patterned anodic aluminum oxide arrays. Refer to Results and Discussion for description of each step.

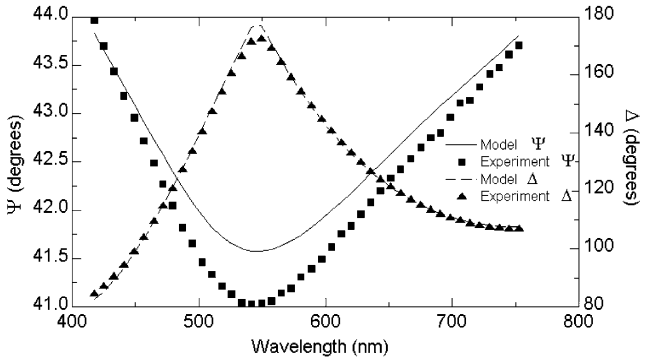

Figure 2. Ellipsometric spectrum collected after deposition of a silica layer on silicon wafers with evaporated aluminum films.

pseudo-optical constants of aluminum were determined with unmodified aluminum slides. The collected ψ and Δ data for aluminum substrates were fit to a parametric model, which included a combination of a Drude oscillator and 6 Lorentz oscillators. These pseudo-optical constants were recorded to a file and used for modeling of the silica layer on the top of aluminum. The determined pseudo-refractive index and extinction coefficient were approximately 10% smaller than the optical constants for aluminum incorporated in the software database. The pseudo-optical constants of metals are known to be sensitive to the presence of surface oxide layers and film evaporation conditions. The ellipsometric spectra for silica-coated slides were analyzed with two one-layer optical models. The first model included the aluminum substrate and a Cauchy layer. The

(22) Rabin, O.; Herz, P. R.; Lin, Y.-M.; Akinwande, A. I.; Cronin, S. B.; Dresselhaus, M. S. *Adv. Funct. Mater.* **2003**, *13*, 631.

Table 1. Results of Analysis of Ellipsometric Data Acquired after Deposition of a Silica Layer on Silicon Wafers

model	spin-coated silica film	annealed silica film
Cauchy thickness, nm	221 ± 2	184 ± 1
Cauchy A	1.436 ± 0.008	1.435 ± 0.002
Cauchy B	(6.9 ± 7.5) × 10^{-4}	(20 ± 6) × 10^{-4}
Cauchy mean-squared error (MSE)	6.5	5.5
EMA thickness, nm	223 ± 2	183 ± 1
EMA fraction of voids, %	6.6 ± 1.2	2.8 ± 0.6
EMA mean-squared error (MSE)	7.6	6.0

Cauchy dispersion relationship, which is frequently used for analysis of transparent films,[23] is defined by eq 1. In this equation, n is refractive index and λ is the wavelength of light in micrometers.

$$n(\lambda) = A + B/\lambda^2 \quad (1)$$

The fit parameters were the thickness of a Cauchy layer and two Cauchy coefficients (A, B). In the second model, the transparent layer on the top of aluminum was modeled with the Bruggeman effective medium approximation (EMA) model as a mixture of silica and voids with the optical constants incorporated in WVASE-32 software. In this case, the fit parameters were the EMA layer thickness and a fraction of voids. The results of regression analysis along with the mean-squared error (MSE) are shown in Table 1 (column 1) for both models. The results of modeling (the first model) are also demonstrated in Figure 2. The experimental ψ does not completely match the model because of a magnified scale on the left Y-axis. Although both one-layer models resulted in similar estimates of the silica layer thickness, the second one was more informative. Although a fraction of voids cannot be considered as an accurate representation of the silica film porosity, it may be used to evaluate how thermal annealing effects the silica films.[23] To obtain less porous silica films and to ensure good adhesion and spreading of a photoresist, silica-coated slides were thermally annealed and subsequently examined by SE. Table 1 (column 2) contains the results of regression analysis for thermally annealed silica films. Comparison of columns 1 and 2 indicates that both the thickness of silica film and fraction of voids decreased upon thermal annealing. The presence of few voids was also confirmed by SEM (dark spots on the left side of Figure 5).

To investigate the ability of silica films (both annealed and as deposited) to serve as a protective barrier for anodization, silica-coated slides were subjected to anodization. Figure 3 shows current transients collected for three slides: bare aluminum, aluminum with a deposited silica film, and aluminum with a thermally annealed silica film. Note that a logarithmic Y-axis is employed instead of the more typically used linear Y-axis. The current transient for anodization of bare aluminum is divided into three regions: formation of the barrier oxide layer, initiation of pore formation, and steady state pore growth (e.g., formation of the porous oxide layer). The formation of pores usually starts after 3−5 min of anodization and is manifest when a plateau (steady-state) current is established. The plateau currents for slides with silica layers were approximately 2 orders of magnitude lower than one for a bare aluminum slide. On the basis of these data, we conclude that the silica layer significantly attenuates anodization of aluminum. From previous research we concluded that the acidic electrolyte can minimally penetrate through silica and reach the silica/aluminum interface via voids. Therefore, the deposited silica film can effectively act as an anodization barrier.[15] This barrier is necessary to prevent pore formation during anodization of aluminum. The silica film not only severely limits the electrolyte access to aluminum, but also acts as a dielectric barrier at which a substantial voltage drop takes place. As a result, the voltage drop in the barrier oxide layer is insufficient to induce dissolution of alumina and pore formation, both of which are electric-field-driven processes. In addition, electrical measurements demonstrate that thermal annealing improves the dielectric property of the silica layer. As shown in

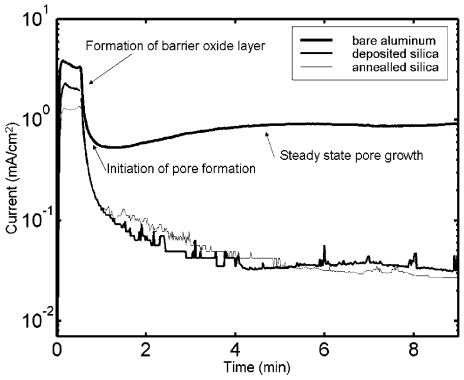

Figure 3. Current transients obtained during anodization: (a) bare aluminum, (b) aluminum with a layer of silica, and (c) aluminum with a thermally annealed layer of silica.

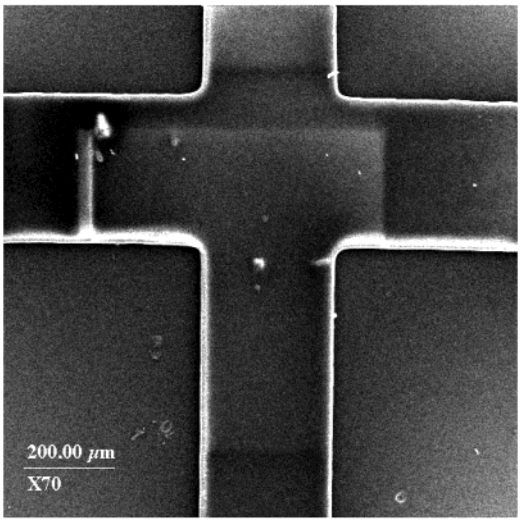

Figure 4. SEM image of a patterned feature. The cross in the middle of slide represents a layer of silica.

(23) Tompkins, H. G.; McGahan, W. A. *Spectroscopic Ellipsometry and Reflectrometry*; John Wiley & Sons: New York, 1999.

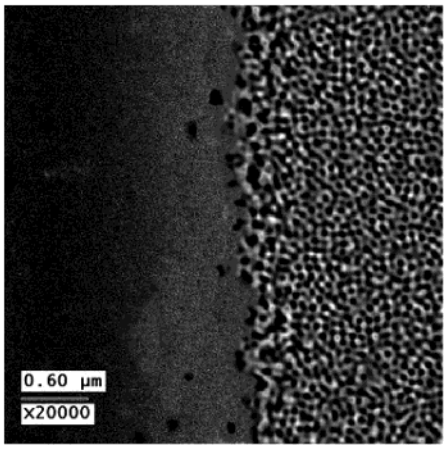

Figure 5. SEM micrograph: the top view of the interface between nanoporous anodic aluminum oxide and aluminum.

Figure 3, the plateau current for the slide with a thermally annealed silica film was somewhat lower than one for the slide with an as-deposited silica film. Thus, thermal annealing, as expected, makes the silica film less porous and a better barrier for anodization.

After the deposition of silica and subsequent thermal annealing, photolithography was employed to pattern the photoresist on the silica-coated slide. Plasma etching was then employed to transfer patterns from the patterned photoresist onto the underlying layer of silica. To control the extent of etching, slides were intermittently removed from the etching chamber, and the silica layer thickness was measured by SE. The cross-section of the incident light beam in the ellipsometer was small enough to sample only those areas that did not contain the patterned photoresist. Etching and subsequent ellipsometric measurements of the silica layer thickness were performed as many times as necessary to remove the silica layer (typically 2 or 3 times). On the basis of these measurements, the average etch rate of silica was approximately 440 nm/min. Etching was considered to be complete when SE spectra collected from etched silica slides closely resembled SE spectra collected from bare aluminum slides. The slide with the patterned layers of silica and photoresist was subjected to the two-step anodization procedure. The patterned layer of photoresist was usually stripped away during treatment with the mixed acid used to etch alumina formed at the first anodization step. However, the patterned layer of silica was preserved even during anodization of aluminum and etching of alumina and acted as the anodization barrier. Figure 4 shows a low-magnification SEM micrograph acquired to demonstrate a patterned feature. The cross pattern in the middle of the slide contains a layer of silica. The typical line width of patterned features on developed slides was about 0.26−0.30 mm. An increase of 4−20% in width of the lines from the original photomask was due to two reasons. First, the UV light was not collimated. Second, the edges of the lines in the photomask pattern were not well defined at high resolution. Because of these two reasons, the edges of the photoresist pattern were not evenly exposed. Using a collimated UV source and a high-resolution photomask, it is possible to reduce the line broadening during the pattern transfer process.

The structure of patterned AAO arrays was investigated by SEM. Figure 5 shows the top view of the interface between aluminum covered with silica (left half of the image) and nanoporous anodic aluminum oxide (clearly seen on the right half of the microphotograph). The roughness of the boundary was due to limitations of the employed photolithography system. In contrast, plasma etching of silica was anisotropic. Thus, the roughness of the boundary was due to rough edges of the patterned photoresist and not the plasma etching process. Figure 5 corresponds to the state of the surface after the completion of all steps described in the procedure and illustrated in Figure 1. The analysis of SEM micrographs confirms that the overall seven-step fabrication process is successful. A clear boundary is observed between two regions, one with pores arranged in an approximately hexagonal order and the other with no pores. The presence of the clear boundary between the two regions indicates that the silica layer acts as an effective dielectric barrier during anodization of aluminum. Employment of silica is advantageous over organic coatings (e.g., photoresists, rubber coatings). Silica demonstrates excellent adhesion to aluminum with a native oxide layer and remains attached to the surface even under severe oxidative conditions in the electrochemical cell. In addition, the fabrication steps (photolithography and plasma etching) are standard, and, therefore, the proposed procedure can be incorporated to a standard fabrication line. The dark spots on the left side of the image are probably due to the presence of voids in the silica layer. More hexagonal pore arrangement could be obtained by depositing thicker aluminum films and, consequently, running anodization for longer periods of time. Detailed investigations of the membrane features and their chemical modifications are ongoing.

Conclusions

In this report, a novel protocol is demonstrated to pattern AAO arrays by using well-established procedures and techniques. A facile approach to fabricate these arrays includes a combination of sol−gel processing, photolithography, plasma etching, and two-step anodization of aluminum. The attractive feature of these AAO arrays is that the regions of the nanoporous anodic aluminum oxide alternate with the regions of aluminum. Therefore, patterned AAO arrays have both enhanced mechanical strength and electrical conductivity. These properties make them advantageous over other AAO arrays. Successful implementation of the seven-step fabrication process relies on application of spectroscopic and electrical measurements and electron microscopy to monitor fabrication steps. Spectroscopic ellipsometry provides a convenient way to determine the thickness of silica layer during processing (e.g., deposition, annealing, and etching). Moreover, monitoring of the silica layer thickness allows us to determine the necessary duration of the fluorocarbon plasma etching. Electrical measurements show that the silica layer deposited by using the sol−gel procedure blocks the pore formation during anodization of aluminum. SEM demonstrates that a clear boundary exist between two regions, one with nanoporous anodic aluminum oxide and the other with aluminum. Fabrication of patterned

AAO arrays with intermittent aluminum supports opens an opportunity to incorporate them into micro- and nanodevices.

Acknowledgment. This work was supported in part by Army Research Office, DEPSCoR grant DAAD190210085, Air Force Office of Scientific Research (F49620-01-1-0168), and the Center for Micro-Engineered Materials, UNM. We thank Corey Bungay (J.A. Woollam Co. Inc., Lincoln, NE) for assistance with interpretation of SE data and Dr. G. V. Ramo Rao for assistance with the sol−gel procedure and discussions at the initial stage of this project. We thank Micromachines Inc., Monrovia, CA for donation of silicon wafers with evaporated aluminum.

CM034553V